ELSEVIER

Journal of Magnetism and Magnetic Materials 182 (1998) 287–296

journal of magnetism and magnetic materials

Critical phenomena in amorphous thin- and ultrathin-film multilayers

Ch.V. Mohan[a,b,*], H. Kronmüller[a]

[a] *Max-Planck Institut für Metallforschung, Institut für Physik, Heisenbergstrasse 1, 70569 Stuttgart, Germany*
[b] *Max-Planck Institut für Mikrostrukturphysik, Am Weinberg 2, 06120 Halle, Germany*

Received 2 June 1997; received in revised form 6 August 1997

Abstract

In order to investigate the magnetic phase transition that occurs at the Curie temperature in magnetic thin- and ultrathin-film multilayers, we have carried out extensive magnetization measurements in the temperature range embracing the critical region on amorphous $(Tb_{0.27}Dy_{0.73})_{0.32}Fe_{0.68}$ thin- and ultrathin-film multilayers separated by magnetic (Cr) or non-magnetic (Nb) interlayers. These data are analyzed by using the conventional methods like the modified Arrott plots, Kouvel–Fisher method, scaling-equation-of-state analysis and the magnetization isotherm at the Curie point and the critical exponents β, γ and δ which describe the phase transition based on the power laws of the spontaneous magnetization, the initial susceptibility and the critical magnetization isotherm, respectively, have been deduced. Depending on the type of the sample, we could see two types of transitions, either characterized by three-dimensional Heisenberg-like critical exponents or two-dimensional Ising-like. The reasons for this are discussed in detail.

PACS: 75.40.Cx; 75.30.Kz; 75.50Kj

Keywords: Magnetic phase transition; Thin-film multilayers; Critical exponents

1. Introduction

It has been a point of interest to see the influence of disorder on the critical behaviour of spin systems that exhibit a second-order magnetic phase transition [1–4]. Though the critical phenomena near the magnetic phase transition temperature have been intriguing the scientific community for quite a long time, there have been only a few detailed studies made on the phase transitions that occur in magnetic thin- and ultrathin-film multilayers, especially in the amorphous ones. Recent studies are based on the interest of scientists to observe a two-dimensional (2D) Ising type of phase transition experimentally [5–8]. A possible realization of a 2D system is a single crystallographically ordered monolayer of magnetic atoms

* Correspondence address: Max-Planck Institut für Mikrostrukturphysik, Am Weinberg 2, 06120 Halle, Germany. E-mail: mohan@mpi-halle.mpg.de.

0304-8853/98/$19.00
PII S0304-8853(97)01046-9

atop a non-magnetic substrate. However, our main interest lies in the phase transitions that occur in amorphous thin- and ultrathin-film multilayers [9–11].

The temperature dependence [12–16] of the spontaneous magnetic polarization, J_S, the initial susceptibility $\chi_0'(T < T_C)$ and $\chi_0(T > T_C)$, and the dependence of the magnetic polarization J on the internal field $\mu_0 H$ at the Curie point are governed by the following relations:

$$J_S \propto (-t)^{\beta}, \quad t < 0, \tag{1}$$

$$\chi_0' \propto (-t)^{-\gamma'}, \quad t < 0, \tag{2}$$

$$\chi_0 \propto (-t)^{-\gamma}, \quad t > 0, \tag{3}$$

$$J \propto H^{1/\delta}, \quad t = 0, \tag{4}$$

where $t = (T - T_C)/T_C$, β, γ, γ' and δ are the critical exponents.

To determine the exponents β and γ, we first apply the modified Arrott plots [17] method based on the Arrott–Noakes equation of state [18], given by

$$(\mu_0 H/J)^{1/\gamma} = (T - T_C)/T_1 + (J/J_1)^{1/\beta},$$

where T_1 and J_1 are the material-dependent parameters. From these plots, the spontaneous magnetic polarization ($J_S(T)$) and the inverse initial susceptibility ($\chi_0^{-1}(T)$) are derived as functions of temperature. The values of the Curie temperature T_C, β and γ are obtained with the help of the Kouvel–Fisher [19] equations

$$J_S(T)[\mathrm{d}J_S(T)/\mathrm{d}T]^{-1} = (T - T_C)/\beta$$

and

$$\chi_0^{-1}(T)[\mathrm{d}\chi_0^{-1}(T)/\mathrm{d}T]^{-1} = (T - T_C)/\gamma.$$

Another independent way to determine the critical exponents β, γ' and γ is by using the scaling theory [20] which predicts the existence of the reduced equation of state of the form

$$J/|t|^{\beta} = f_{\pm}(\mu_0 H/|t|^{\beta+\gamma}).$$

This relation further implies that $J/|t|^{\beta}$ as a function of $\mu_0 H/|t|^{\beta+\gamma}$ falls on two different curves, one for temperatures below and the other for temperatures above the Curie point. The exponent δ can be obtained from the slope of the $\ln J$ versus $\ln(\mu_0 H)$ plot at the Curie temperature (Eq. (4)).

Another way to analyze the phase transitions is with the help of a non-linear temperature variable defined as $t' = (T - T_C)/T$. This was shown to be a highly fruitful way by Souletie and Tholence [21] regarding the discovery that the initial susceptibility of crystalline Ni varies with temperature in accordance with a modified power-law $\chi_0 \propto (1/T)(-t')^{-\gamma^*}$, $t > 0$. This relation was shown to be valid over a wide range of temperatures extending up to $3T_C$. This type of results were also shown in Heisenberg spin systems with localized moments [22] which means that this power law holds good for systems with both itinerant and localized electrons. γ^*, though it has the same value in a very broad temperature range (up to $3T_C$), at high temperatures its value depends on the coordination number and the value of spins localized at lattice sites of the three-dimensional system in question. Though the use of non-linear temperature variable promises interesting physics, we have not tried to analyze our data using this, as our data are very much limited to within the critical region and it will be interesting to use the non-linear temperaure variable only if the measurements are performed up to very high temperatures which is not the case with our data.

2. Experimental details

We have studied three different samples of the same nominal composition in this work. The first one (sample 1) comprises of Cr/$(Tb_{0.27}Dy_{0.73})_{0.32}Fe_{0.68}$ thin film multilayers with the Cr layer thickness and Tb–Dy–Fe layer thickness approximately equal to 10 and 100 Å, respectively. The second one (sample 2) consists of Cr/$(Tb_{0.27}Dy_{0.73})_{0.32}Fe_{0.68}$ multilayers with thickness of the Cr and Tb–Dy–Fe layers, respectively, equal to 10 and 10 Å and the third one (sample 3) is a Nb/$(Tb_{0.27}Dy_{0.73})_{0.32}Fe_{0.68}$ multilayer system with the thickness of Nb and Tb–Dy–Fe layers equal to 100 and 10 Å, respectively. The reasons for choosing such a high value for the Nb layer thickness are explained in the next part of the paper. All these samples contain 100 bi-layers and they are prepared by the RF sputtering technique. All the

samples were capped by a Nb layer of thickness 500 Å. We have used sapphire as the substrate material which has offered a flat surface for the sample deposition. The composition and the amorphous nature of these samples are confirmed by the EDAX and high-resolution electron microscopy techniques. The sample preparation and characterization procedures are discussed in detail in Refs. [9–11,23,24]. Magnetic polarization measurements are performed on a pile of few pieces of the sample by a quantum design SQUID magnetometer (Model: MPMS). Magnetization values are measured as a function of field (up to 10 kOe) at various temperature values (at 0.25 K steps) on either side of the Curie point. The demagnetization factor is estimated from the low-field magnetization data and demagnetization corrections are made.

The composition $(Tb_{0.27}Dy_{0.73})_{0.32}Fe_{0.68}$ is well known as giant magnetostrictive material [25]. The intermetallic alloys $TbFe_2$ and $DyFe_2$ are characterized by large values for the magnetostriction and also large values for the crystal anisotropies K_i. The origin of both these effects is the strong spin–orbit coupling between the electron spins and the anisotropic charge distribution. On the other side, there is a change of sign K_1 between $TbFe_2$ (positive) and $DyFe_2$ (negative) at the exact composition $(Tb_{0.27}Dy_{0.73})_{0.32}Fe_{0.68}$. Amorphous and nanocrystalline materials of the composition $(Tb_{0.27}Dy_{0.73})_{0.32}Fe_{0.68}$ can therefore exhibit at the same time large magnetostriction and low coercivity and are well-promising candidates for magnetostrictive applications. The main motivation for the present study was to investigate the magnetic phase transition in such thin- and ultrathin-film multilayers and check their critical behaviour.

3. Results, data analysis and discussion

3.1. Sample 1

The modified Arrott plot isotherms constructed from the recorded magnetization data are shown in Fig. 1. The choice of the exponent values used to construct these plots is chosen [26–28] in such a way that the $J^{1/\beta}$ versus $(H/J)^{1/\gamma}$ isotherms over a maximum possible temperature range around the Curie temperature are straight and parallel. The linearity of these isotherms in the high-field region and the finding that they are approximately parallel to one another guarantees that the exponents β and γ determined are accurate to within $\pm 5\%$ [17]. The temperature dependence of J_S and χ_0^{-1} obtained from the extrapolation methods [17], is depicted in Figs. 2 and 3, respectively. From these

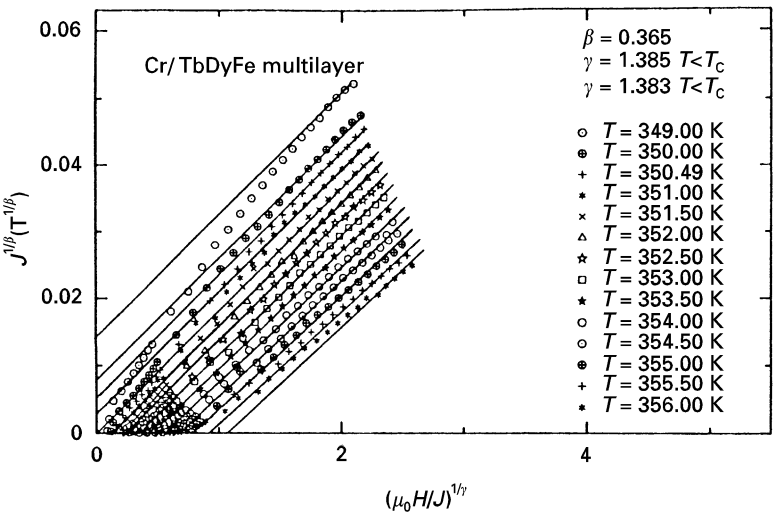

Fig. 1. Modified Arrott plot isotherms constructed from the magnetization data on sample 1 in a narrow temperature range around the Curie temperature. The exponent values used to construct these plots are also shown.

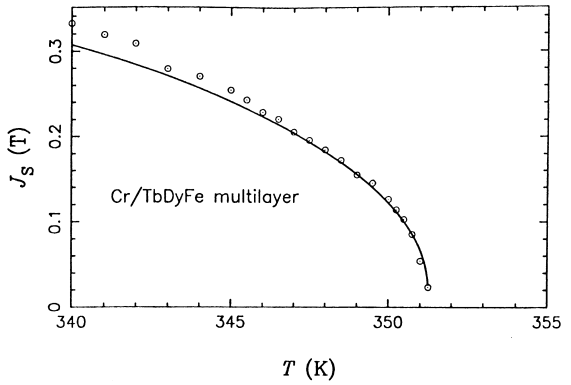

Fig. 2. The temperature variation of the spontaneous magnetic polarization for sample 1. The solid line through the data points represents the fit based on the power law.

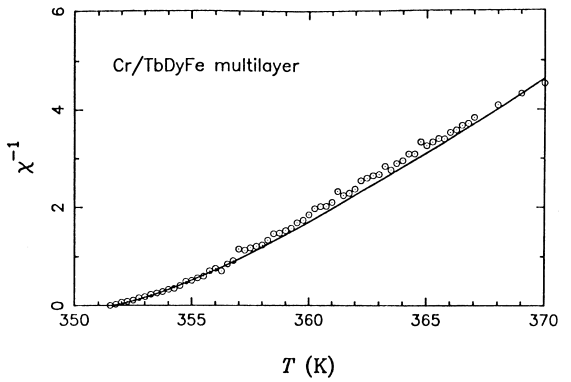

Fig. 3. The inverse initial susceptibility for sample 1 plotted as a function of temperature. The solid line through the data points represents the fit based on the power law.

data, the quantities $J_S(T)[dJ_S(T)/dT]^{-1}$ and $\chi_0^{-1}(T)[d\chi_0^1(T)/dT]^{-1}$ are computed and are plotted against temperature in Fig. 4a and Fig. 4b, respectively. The straight lines in these figures represent the best least-squares fits to the data based on the Kouvel–Fisher equations.

The scaling plots corresponding to the sample 1 are shown in Fig. 5. A very good collapse of the magnetization data at various field values onto two different curves indicates that the values of the Curie temperature and the exponents are sufficiently accurate [17].

The ln J versus ln($\mu_0 H$) plots were also constructed and are shown in Fig. 6. The straight line in this figure shows a fit to the data at the Curie temperature based on Eq. (4).

Now the values of the critical exponents obtained for sample 1 are $\beta = 0.36 \pm 0.02$, $\gamma' = \gamma = 1.38 \pm 0.03$ and $\delta = 4.87 \pm 0.20$. The value of δ calculated from the scaling law $\gamma' = \gamma = \beta(\delta - 1)$ [29] with the help of γ', γ and β values deduced from the earlier methods is equal to 4.83 ± 0.2, which is in close agreement with the value obtained from the ln J versus ln($\mu_0 H$) plot at T_C. These values are also in good agreement with those ($\beta = 0.365$, $\gamma = 1.386$ and $\delta = 4.800$) for a three-dimensional Heisenberg spin system with nearest-neighbour interactions, as predicted by the renormalization group calculations [30–34]. It is seen that the exponent values obtained via various methods are very consistent.

Observation of 3D Heisenberg-like critical exponents for the case of the above sample is definitely not unexpected. This is just because each of the Tb–Dy–Fe layers of 100 Å thickness is enough to represent a system of lattice dimensionality of three and hence the exponents assume values close to the bulk values which are normally 3D Heisenberg-like.

3.2. Sample 2

The thickness of each of the Tb–Dy–Fe layers for sample 2 is maintained to be approximately 10 Å which is thin enough to approach a lattice of reduced dimensionality as this value falls in the monolayer range. We have followed the same procedure as in the case of sample 1 to deduce the critical exponents. However, we show only a few important plots regarding this.

The ln J versus ln($\mu_0 H$) plots are shown in Fig. 7. The straight line fit to the data at the Curie temperature based on Eq. (4) is also shown. The critical exponents obtained for sample 2 are $\beta = 0.36 \pm 0.02$, $\gamma' = \gamma = 1.38 \pm 0.03$ and $\delta = 4.77 \pm 0.20$. The scaling plots corresponding to sample 2 are shown in Fig. 8. Again it is found that the values of the exponents are in good agreement with those for a 3D Heisenberg spin system.

Now, we shall concentrate on our result that the magnetic phase transition in sample 2 has been characterized by 3D Heisenberg-like critical exponents. The thickness of each of these films is thin

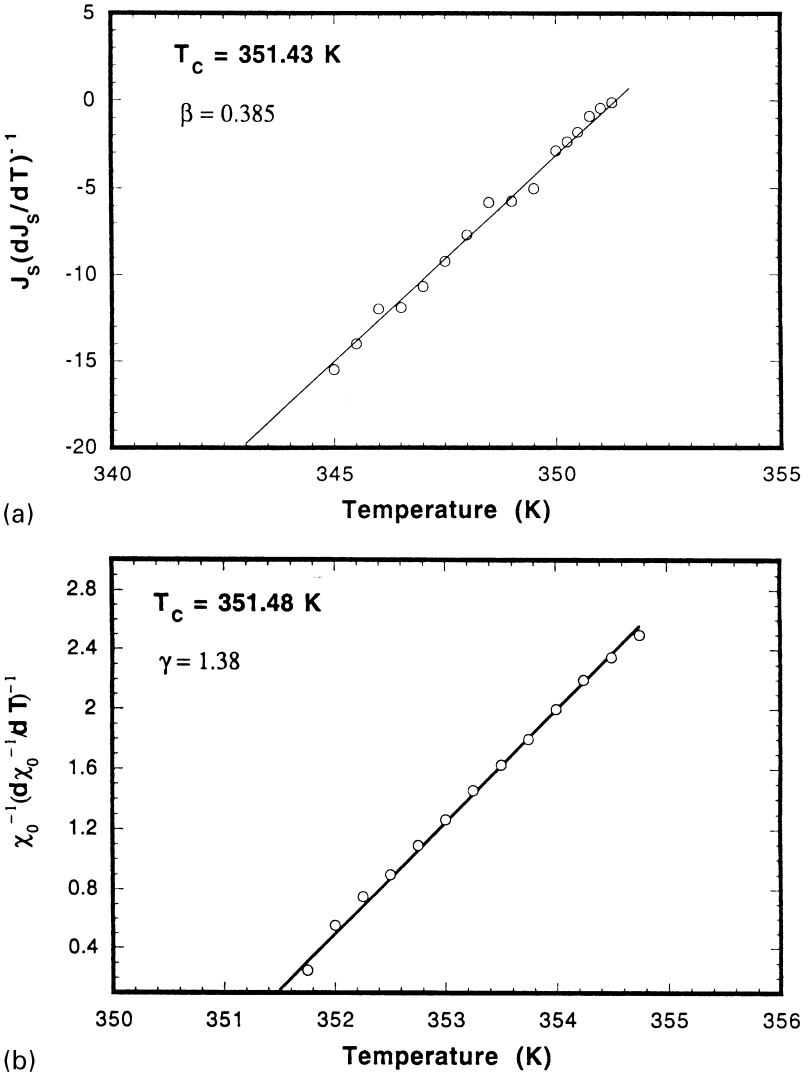

Fig. 4. (a) Kouvel–Fisher plot for β for sample 1. The straight line is based on the Kouvel–Fisher equation for β. (b) Kouvel–Fisher plot for γ for sample 1. The straight line is based on the Kouvel–Fisher equation for γ.

enough to represent systems with lattice dimensionality of two when considered individually. However, since we have used Cr as the interlayer to separate these films, this induces some magnetic exchange interactions between adjacent layers [35] and the whole system is magnetically connected and hence we obtain 3D Heisenberg-like critical exponents.

3.3. Sample 3

With a view to avoid the magnetic interactions induced by the interlayer, we have now chosen, in sample 3, Nb as the interlayer material. We have also chosen a very high value for the thickness of Nb layers in order to ensure an absolute isolation of the magnetic layers (now only Tb–Dy–Fe layers).

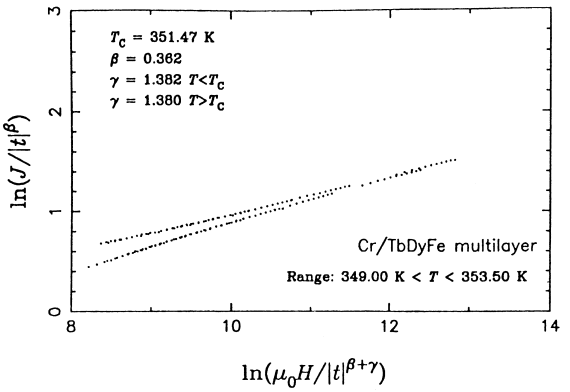

Fig. 5. Scaling plots corresponding to sample 1. The details of the parameters used to construct these plots are also shown.

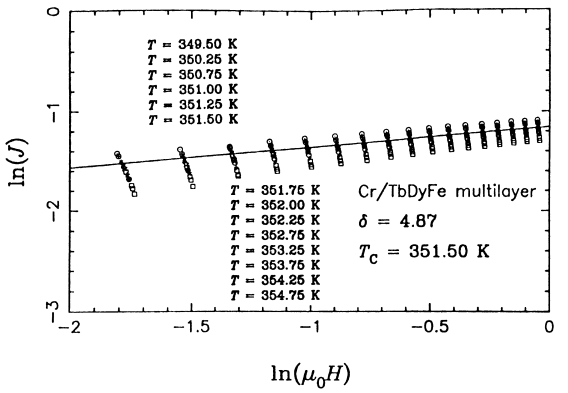

Fig. 6. The ln J versus ln($\mu_0 H$) plots for sample 1. The straight line indicates the fit to the data at the Curie temperature based on Eq. (4). The value of the exponent is also shown.

We have again repeated all our experiments and analyzing procedures as explained earlier. The spontaneous magnetic polarization and the initial inverse susceptibility are plotted in Figs. 9 and 10, respectively, as functions of temperature. The transition in this sample is found to be very sharp compared to the earlier samples and is also characterized by different values of the critical exponents. It was not possible with these data to obtain good Kouvel–Fisher plots as the transition is very sharp and hence we were left with very few points in the temperature range close to the Curie temperature. The fits obtained for these data based on Eqs. (1) and (2) are shown as continuous curves in Figs. 9 and 10. The values of the critical exponents obtained in this way are $\beta = 0.126 \pm 0.020$ and $\gamma = 1.752 \pm 0.030$. The ln J versus ln($\mu_0 H$) plots were also constructed and are shown in Fig. 11. The straight line fit to the data at the Curie temperature based on Eq. (4) is also shown.

Now the values of the critical exponents obtained for sample 3 are $\beta = 0.126 \pm 0.02$, $\gamma' = \gamma = 1.75 \pm 0.03$ and $\delta = 15.12 \pm 1.00$ (Widom scaling law yields $\delta = 15.00$). We have again constructed the scaling plots with these values of the critical exponents (Fig. 12) and we see an excellent plot of the data in which all the data corresponding to various field values and temperatures fall on two different curves. These values of the critical exponents are also found to be in excellent agreement with those predicted for a 2D Ising model [36–40] ($\beta = 0.125$, $\gamma = 1.750$ and $\delta = 15.00$).

It is very interesting to see such values for the critical exponents in the system under study. However, these values could very well be explained based on the following arguments. The amorphous nature of our samples ensures the absence of perfect translational symmetry. Though Fe does not have ideally localized spins, the rare-earth moments are localized and probably this would satisfy the condition as desired by the Ising Hamiltonian. The values of the exponents could also be explained based on the fact that the numerical values of the critical exponents depend only on (i) the lattice dimensionality of the spin system, (ii) the number of components of the order parameter, (iii) the symmetry of the Hamiltonian and (iv) the range of the microscopic interactions (mainly exchange) responsible for the phase transition. Although the presence of defects is expected [41] to alter the universality class of the phase transition, this is not true with the sample under investigation probably because the correlation length is much larger than the distance between the defects [42].

4. Summary and conclusions

We have made a detailed study on the magnetic phase transition which occurs at the Curie temperature by characterizing it with the help of the

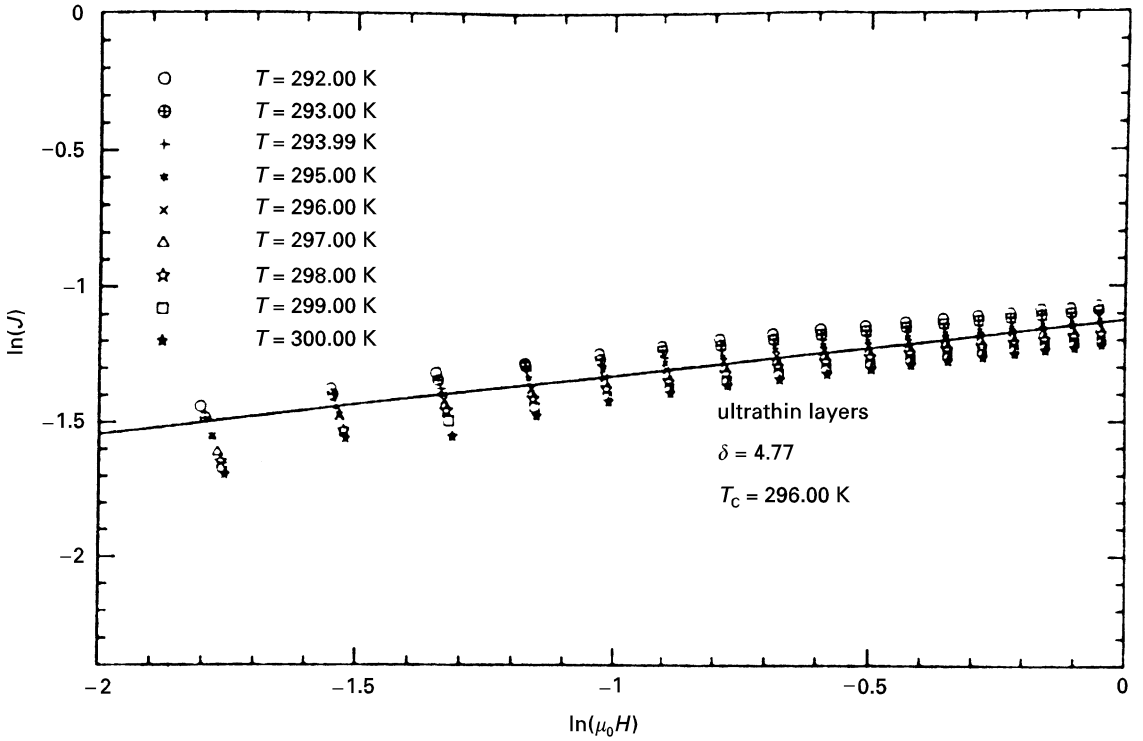

Fig. 7. The ln J versus $\ln(\mu_0 H)$ plots for sample 2 in a narrow temperature range around the Curie point.

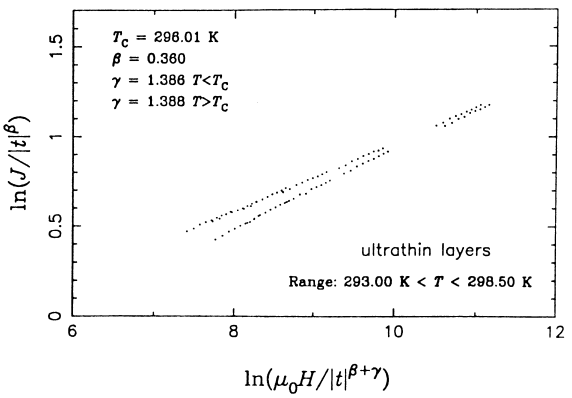

Fig. 8. Scaling plots for sample 2.

critical exponents in a system of amorphous thin- and ultrathin-film multilayers. Extensive magnetization measurements have been performed in the critical region of three samples of same composition ($(Tb_{0.27}Dy_{0.73})_{0.32}Fe_{0.68}$ thin- and ultrathin-film multilayers) with the number of layers being identical for all the samples but with the Tb–Dy–Fe layers of varying thickness separated either by magnetic (Cr) or non-magnetic (Nb) interlayers. Conventional methods have been used to analyze the phase transition and the results obtained are summarized as follows:

- The phase transition in the Cr/$(Tb_{0.27}Dy_{0.73})_{0.32}Fe_{0.68}$ multilayer system with the Cr and $(Tb_{0.27}Dy_{0.73})_{0.32}Fe_{0.68}$ layer thickness equal to 10 and 100 Å, respectively, is characterized by 3D Heisenberg-like critical exponents.
- The critical exponents for the Cr/$(Tb_{0.27}Dy_{0.73})_{0.32}Fe_{0.68}$ system containing 100 layers with the thickness of the Cr and the $(Tb_{0.27}Dy_{0.73})_{0.32}Fe_{0.68}$ layers equal to 10 and 10 Å are also close to the 3D Heisenberg values reflecting the magnetic interaction induced by Cr.

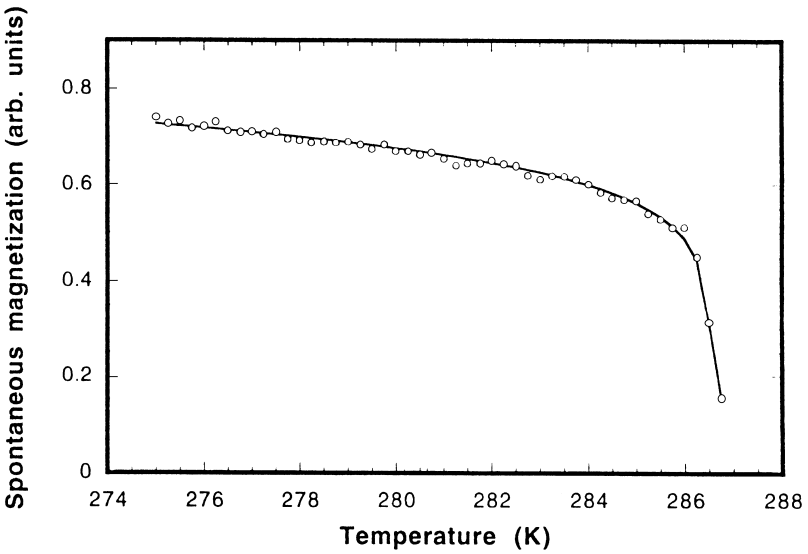

Fig. 9. Temperature dependence of the spontaneous magnetic polarization for sample 3. The continuous line through the data points indicates the fit to the data based on the power law given by Eq. (1) and with a value of $\beta = 0.126$.

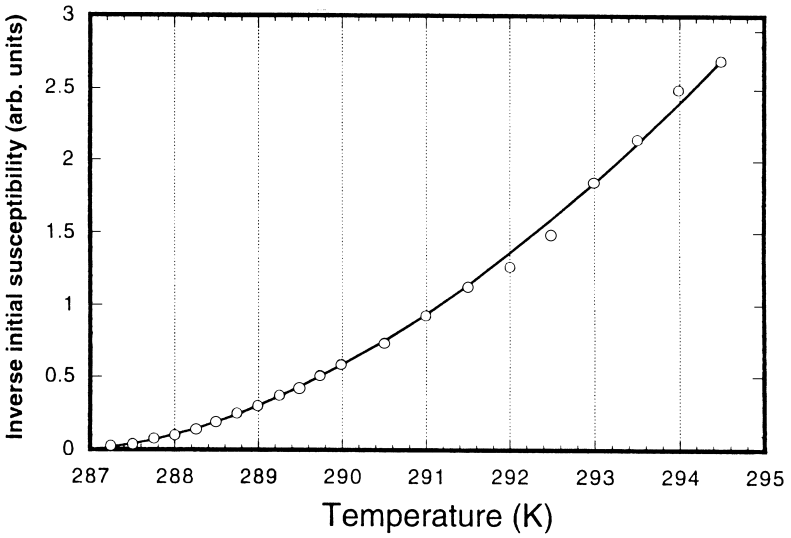

Fig. 10. Temperature dependence of the inverse initial susceptibility for sample 3. The continuous line through the data points indicates the fit based on Eq. (3) of the text and with a value for $\gamma = 1.752$.

- We obtain 2D Ising-like critical exponents for the Nb/$(Tb_{0.27}Dy_{0.73})_{0.32}Fe_{0.68}$ multilayer system with the thickness of the Nb and $(Tb_{0.27}Dy_{0.73})_{0.32}Fe_{0.68}$ layers equal to 100 and 10 Å, respectively. Our samples being amorphous in nature prove that the correlation length cannot be limited by the sample inhomogeneities; in other words, the correlation length is much larger than the distance between the defects.

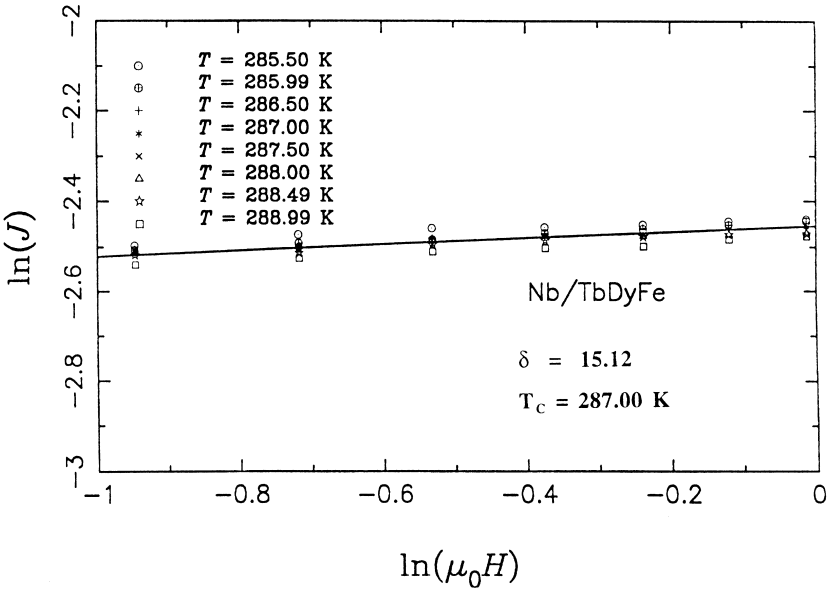

Fig. 11. The ln J versus ln($\mu_0 H$) plots for sample 3 for a few temperature values around the Curie temperature. The straight line in the figure represents the fit yielding the exponent δ.

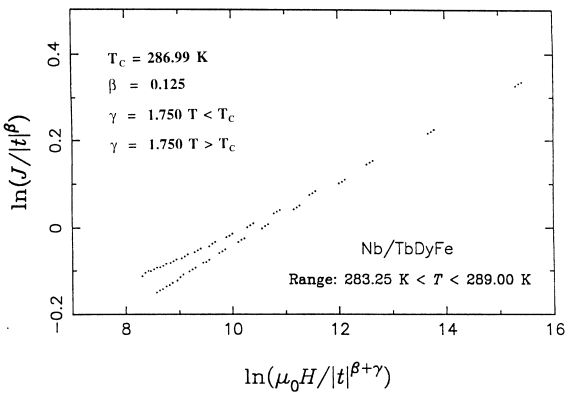

Fig. 12. Scaling plots for sample 3. The values of T_C, β and γ are also shown.

References

[1] M.E. Fisher, Phys. Rev. 176 (1968) 257; R.A. Dunlap, A.M. Gottlieb, Phys. Rev. B 23 (1981) 6106.
[2] R. Birgeneau, J. Als-Nielsen, G. Shirane, Phys. Rev. B 16 (1977) 280.
[3] C. Hohenemser, T.A. Kachnowski, T.K. Bergstresser, Phys. Rev. B 13 (1976) 3154.
[4] R.M. Suter, C. Hohenemser, J. Appl. Phys. 50 (1979) 1814.
[5] C.H. Back, C. Würsch, D. Pescia, Z. Phys. B 98 (1995) 69.
[6] M. Farle, K. Baberschke, Phys. Rev. Lett. 58 (1987) 511.
[7] W. Dürr, M. Taborelli, O. Paul, R. Germar, W. Gudat, D. Pescia, M. Landolt, Phys. Rev. Lett. 62 (1989) 206; J.C. Campuzano, M.S. Foster, G. Jennings, R.F. Wills, W. Unertl, Phys. Rev. Lett. 54 (1985) 2684
[8] H.J. Elmers, J. Hanschild, U. Gradmann, Phys. Rev. B 54 (1994) 15224 and references cited therein.
[9] Ch.V. Mohan, H. Kronmüller, Phys. Stat. Sol. (b) 199 (1997) 563.
[10] Ch.V. Mohan, H. Kronmüller, Phys. Rev. Lett (1997), submitted.
[11] Ch.V. Mohan, M. Seeger, H. Kronmüller, J. Magn. Magn. Mater. 174 (1997) 89.
[12] H.E. Stanley, in: Introduction to Phase Transitions and Critical Phenomena, Clarendon, Oxford, 1971 and references cited therein.
[13] M. Haug, M. Fähnle, H. Kronmüller, F. Haberey, J. Magn. Magn. Mater. 69 (1987) 163 and references cited therein.
[14] M. Seeger, H. Kronmüller, J. Magn. Magn. Mater. 78 (1989) 393.
[15] Y. Shen, I. Nakai, H. Maruyama, O. Yamada, J. Phys. Soc. Japan 54 (1985) 3915.
[16] O. Boxberg, K. Westerholt, Phys. Rev. B 50 (1994) 9331.
[17] S.N. Kaul, J. Magn. Magn. Mater. 53 (1985) 5.
[18] A. Arrott, J.E. Noakes, Phys. Rev. Lett. 19 (1967) 786.
[19] J.S. Kouvel, M.E. Fisher, Phys. Rev. A 136 (1964) 1626.

[20] S. Milosevic, H.E. Stanley, Phys. Rev. B 5 (1972) 2526; S. Milosevic, H.E. Stanley, Phys. Rev. B 6 (1972) 986.
[21] J. Souletie, J.L. Tholence, Solid State Commun. 48 (1983) 407.
[22] E. Carré, J.P. Renard, J. Souleite, J. Magn. Magn. Mater. 54–57 (1986) 697; M. Fähnle, J. Souletie, J. Phys. C 17 (1984) L469.
[23] B. Winzek, Diploma Thesis, University of Stuttgart, 1996, unpublished.
[24] B. Winzek, H. Kronmüller, unpublished results, 1996.
[25] A.E. Clark, Magnetostrictive Rare-earth–Fe2 compounds, in: E.P. Wohlfarth (Ed.), Ferromagnetic Materials, vol. 1, North-Holland, Amsterdam, 1980, p. 531.
[26] Ch.V. Mohan, H. Kronmüller, J. Magn. Magn. Mater. 163 (1996) 96.
[27] A.A. Coelho, Ch.V. Mohan, S. Gama, H. Kronmüller, J. Magn. Magn. Mater. 163 (1996) 87.
[28] S.N. Kaul, Ch.V. Mohan, Phys. Rev. B 50 (1994) 6157.
[29] B. Widom, J. Chem. Phys. 43 (1965) 3892.
[30] V. Privman, P.C. Hohenberg, A. Aharony, in: C. Domb, J.L. Lebowitz (Eds.), Phase Transitions and Critical Phenomena, vol. 14, Academic, New York, 1991, p. 1.
[31] S.N. Kaul, IEEE Trans. Magn. 20 (1984) 1290.
[32] S.N. Kaul, P.D. Babu, Phys. Rev. B 45 (1992) 295.
[33] W.U. Kellner, M. Fähnle, H. Kronmüller, S.N. Kaul, Phys. Stat. Sol. (b) 144 (1987) 397.
[34] P. Hargraves, R.A. Dunlap, J. Phys. F 18 (1988) 553.
[35] P. Grünberg, R. Schreiber, Y. Pang, M.B. Brodsky, H. Sowers, Phys. Rev. Lett. 57 (1986) 2442; M.N. Baibich, J.M. Broto, A. Fert, F. Nguyen van Dau, F. Petroff, P. Etienne, G. Creuzet, A. Friedrich, J. Chazelas, Phys. Rev. Lett. 61 (1988) 2472; G. Pannaccione, F. Sirotti, E. Narducci, G. Rossi, Phys. Rev. B 55 (1997) 389 and references cited therein; S. Mirbt, I.A. Abrikosov, B. Johansson, H.L. Skriver, Phys. Rev. B. 55 (1997) 67.
[36] E.J. Samuelsen, J. Phys. Chem. Solids 35 (1974) 785.
[37] C. Rau, Appl. Phys. A 49 (1989) 579.
[38] S.D. Bader, J. Magn. Magn. Mater. 100 (1991) 440.
[39] Z.Q. Qiu, J. Pearson, S.D. Bader, Phys. Rev. Lett 67 (1991) 1646.
[40] K. Binder, in: C. Domb, M.S. Green (Eds.), Phase Transitions and Critical Phenomena, Academic, London, 1976.
[41] A. Kumar, H.R. Krishnamurthy, E.S.R. Gopal, Phys. Rep. 98 (1983) 57.
[42] C.H. Back, Ch. Würsch, A. Vaterlaus, U. Ramsperger, U. Maier, D. Pescia, Nature 378 (1995) 597.